MELCOR

Further Development Phase-1: 2013–2017 and Phase-2: 2017–2021

Author und Co-author(s)	Bernd S. Jäckel, Leticia Fernandez-Moguel, Terttaliisa Lind
Institution	Paul-Scherrer-Institut
Address	5232 Villigen PSI
Phone, E-mail, Internet address	+41 56 310 2658, bernd.jaeckel@psi.ch, www.psi.ch/sacre
Duration of the Project	2017–2021

ABSTRACT

Full scale experiments conducted in 2011 and 2012 at the Sandia National Laboratories in the Sandia Fuel Project [1] have shown that nitrogen plays an active role in the degradation process of spent fuel cladding materials and may lead to the loss of the only barrier for the fission product release in case of a spent fuel storage accident. To account for the effect of nitrogen in the cladding degradation, PSI carried out experimental investigations in the project Phase-1 accompanied by extensive analyses of the results, and formulation of a conceptual nitriding model in 2013–2017. In Phase-2 of the project in 2017–2021, it is foreseen to complement coding of the model to acquire a stand-alone model for cladding nitriding, as well as to include further cladding degradation by re-oxidation of the nitrided cladding. Once the stand-alone model is available, separate effect tests and integral tests under air oxidation will be used to validate the model. In this report, we summarize the main results of Phase-1 of the project as well as describe the results of the first six months of Phase-2.

In Phase-1, more than 70 separate effect tests were conducted by a PSI PhD student at Karlsruhe Institute of Technology (KIT), Germany. The results of the tests provide a data base sufficient for the development of a nitriding and re-oxidation model to describe the accelerated degradation of cladding materials under air ingress conditions during a severe nuclear accident. The samples were analysed not only for the mass gain during exposure to alternately oxygen, nitrogen, and again oxygen, but also for the composition after the tests using a combined metallographic and image analysis. In addition, detailed examination of the samples was carried out to determine possible existence of Zr-oxy-nitrides as a result of the nitriding reaction. Conceptual model for nitriding includes formation of Zr-oxide and oxygen stabilized α-Zirconium $\alpha Zr(O)$ during pre-oxidation in oxygen, fast nitriding and slow nitriding during the exposure to nitrogen, and the effect of break-away oxidation.

In Phase-2, the conceptual model will be incorporated in the PSI air oxidation and break-away model [2]. At the end of the development, the model will include the nitriding process under oxygen and steam starvation conditions and the strongly accelerated process of re-oxidation when oxygen or steam is recovered as observed in several separate effect tests and also integral experiments such as QUENCH-16, QUENCH-18, and the Sandia Fuel Project tests (SFP). The model will distinguish between two regimes, the break-away regime at temperatures below 1050 °C and the non-break-away regime above 1050 °C. In the high temperature regime the acceleration of the oxidation is based on the morphology change due to the nitriding reaction (porous structure of ZrN).

Project goals

The presence of air can lead to accelerated oxidation of the Zircaloy cladding compared with that in steam, Figure 1, if nitrogen can attack the cladding during oxygen or steam starvation. The models available in the present severe accident codes have mostly very limited description of the effect of nitrogen on the cladding degradation, if any. The missing models lead not only to underestimation of the cladding degradation but also to underestimation of the produced chemical energy. This is especially important for accidents under low nuclear decay heat, e.g., spent fuel pool accidents. Also the dry storage under air cooling or using nitrogen as inertizing cooling gas may lead to cladding degradation at relatively low temperatures due to the effect of nitrogen.

In this work, a model is developed to describe the effect of nitrogen on the Zircalloy cladding degradation when the cladding is exposed to nitrogen under, e.g., air ingress conditions. Until recently, nitrogen was presumed not to react with the cladding materials even under severe accident conditions. Later, it was described as having a catalysing effect thereby accelerating the reactions which lead to cladding oxidation. Now it is acknowledged that under certain conditions, nitrogen takes part in the reactions being a reactant leading to formation of ZrN, and possibly Zr-oxynitrides.

For any considerable formation of ZrN, the prior formation of oxygen stabilized α-Zirconium αZr(O) is needed. The formation of αZr(O) takes place under oxygen starved atmosphere. The effect of Zr-nitride formation is two-fold. Firstly, it forms a mechanically porous structure thereby transforming the protective oxide layer into non-protective, porous layer. The possible subsequent oxidation of the nitride layer, Fig. 1, results in massive failure of the cladding. And secondly, the reactions leading to the cladding degradation in the presence of nitrogen are exothermic and add to the reaction heat released in the process thereby increasing the temperature of the cladding.

For the model development, a series of separate effect tests were carried out to determine the reactions and reaction rates in the different phases of the nitriding and re-oxidation process. The tests were conducted in a thermogravimetric facility using Zircalloy samples which were open on both ends, Fig. 1. The mass gain during pre-oxidation in oxygen, nitriding in nitrogen, and re-oxidation in oxygen was measured and the mass gain rate determined. After the tests, metallographic analyses were carried out to determine the morphology of the different composition regions in the samples. In addition, the relative concentration of different compounds was determined using image analysis. Extensive analyses were carried out to explore the possible presence of Zr-oxynitrides which might have been formed during the experiments to evaluate if these compounds should be taken into account in the model development.

In this reporting period, Phase-1 of the project ended and Phase-2 started. The goals of Phase-1 were:

1) to finish the analysis of the separate effect tests to formulate the conceptual model for cladding nitriding

2) to identify the main mechanisms in the process of cladding nitriding, and

3) to assess the uncertainty of the data from the separate effect tests.

Further goals for Phase-2 in this reporting period were:

4) to evaluate the data available to make a model for re-oxidation

5) to make the first formulation of the nitriding model.

After some deliberation it was deemed useful to combine the two tasks as partly the same formulations and reaction rates can be used for both pre-oxidation processes needed for the nitriding model and re-oxidation. Therefore, the goal for this reporting period was to formulate the global model for

Figure 1:
Cladding (a) oxidation followed by nitriding (b) and re-oxidation (c)
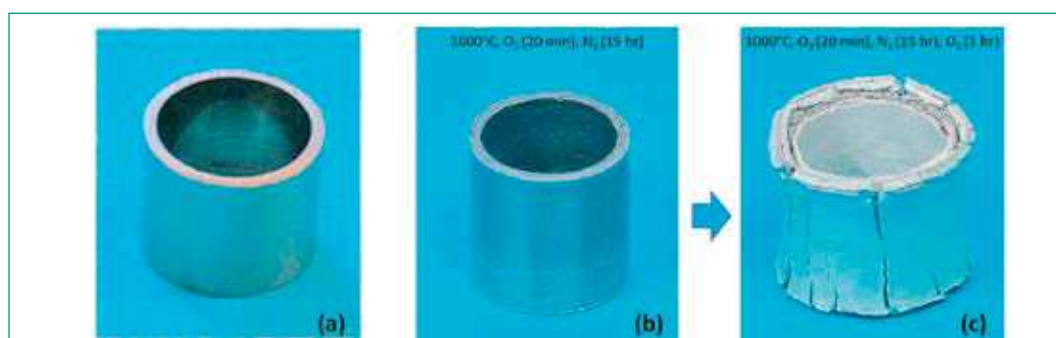
the effect of nitrogen on cladding degradation, and to identify the next step in the model development.

Work carried out in Phase-1

More than 70 thermogravimetric experiments were carried out [3] under alternating exposure to oxygen, nitrogen, and again oxygen to determine the main mechanisms affecting the cladding degradation, and to determine the reaction rates for the different mechanisms in the temperature range 900°C–1200°C. Comparisons of the thermogravimetric results and metallographic investigations were made to support the interpretation of the results. These comparisons [4] showed that the temperature range should be divided into two regions showing significantly different behaviour: i) The low temperature regime below 1050°C in which the oxide layer thickness above a critical value often leads to breakaway of the oxide layer at the cladding surface, and ii) the high temperature regime above 1050°C in which break-away oxidation has not been observed to occur.

The temperature regions were determined partly due to difference in the nitriding reaction rates observed for the two regimes, but mainly based on image analysis. In the tests, the samples were first pre-oxidized under oxygen and then exposed to pure nitrogen with Ar carrier gas. In the low temperature tests at 900°C and 1000°C, the ZrN was formed invariably close to the interface between the Zr metal and the Zr-oxide layer, and ZrN was never found outside of this region. In the high temperature tests at 1100°C and 1200°C, ZrN was found on the outer surface of the oxide layer, at the interface between the metal and the oxide, and also as precipitates inside the oxide layer, Figure 2. The ZrN structure cannot be shown to be a result of the break-away oxidiation, and consequently, the division of the temperature range into two is supported by two different phenomena, i) the occurrence of the break-away oxidation, and ii) the structure of the nitride layer.

Based on the separate effect tests, a model following the scheme shown in Fig. 3 was developed.

Low temperature region < 1050°C

Low temperature region is further divided into non-break-away and break-away region. The break-away criteria are taken from the PSI Air oxidation model of Birchley [5].
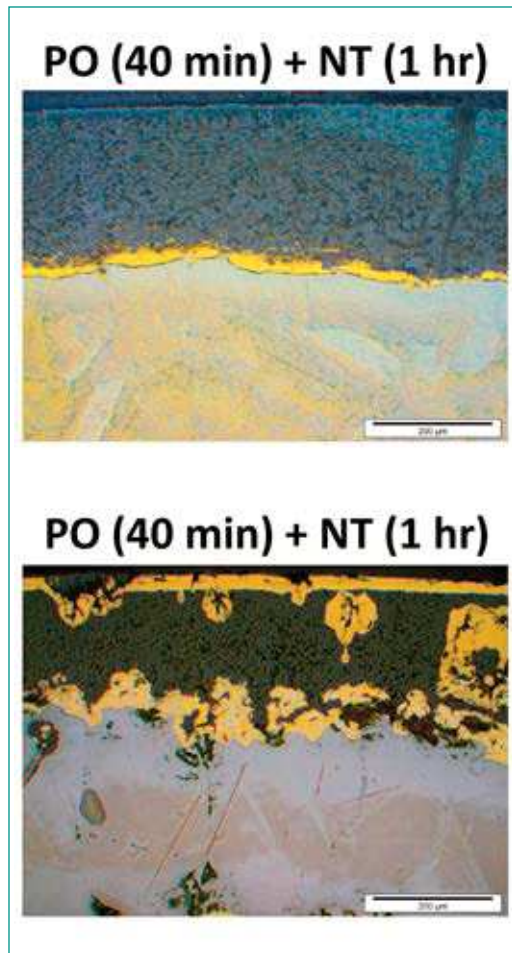
Non-break-away region

During pre-oxidation, a layer of Zr-oxide is formed on the metal sample surface. The comparison of the oxidation rates with the correlation of Uetsuka and Hofmann for the cladding oxidation with oxygen [9] shows good agreement, Figure 4. In addition to the oxide layer formation, oxygen diffuses
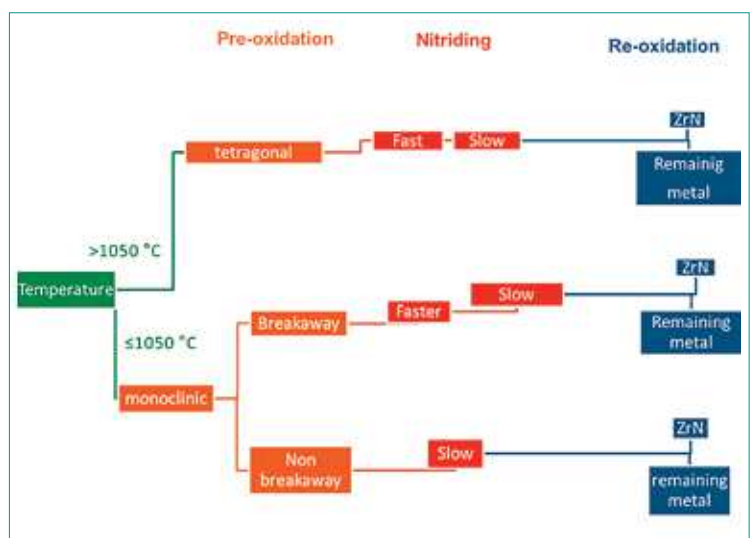

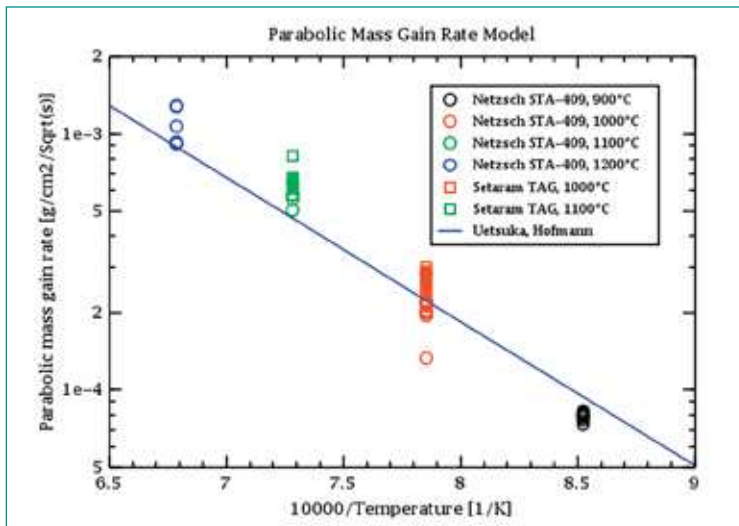**Figure 3:** *The model structure and mechanisms of pre-oxidation, nitriding and re-oxidation*

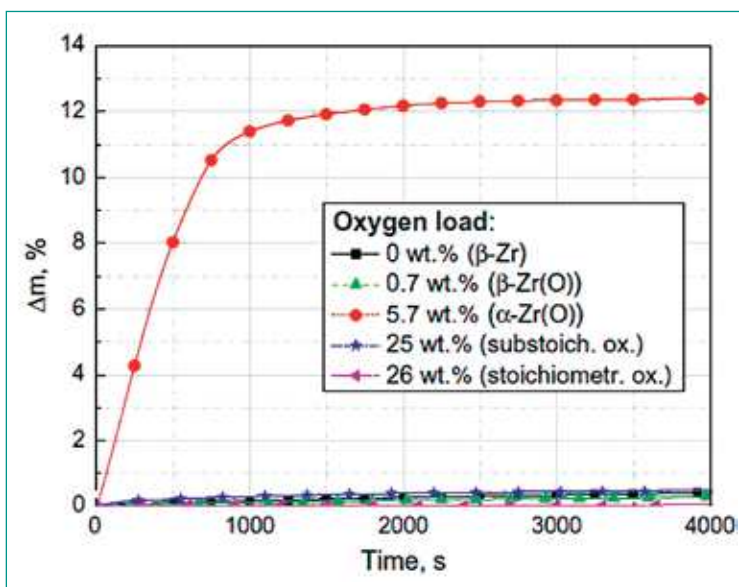Figure 4: *Mass gain rate during pre-oxidation*

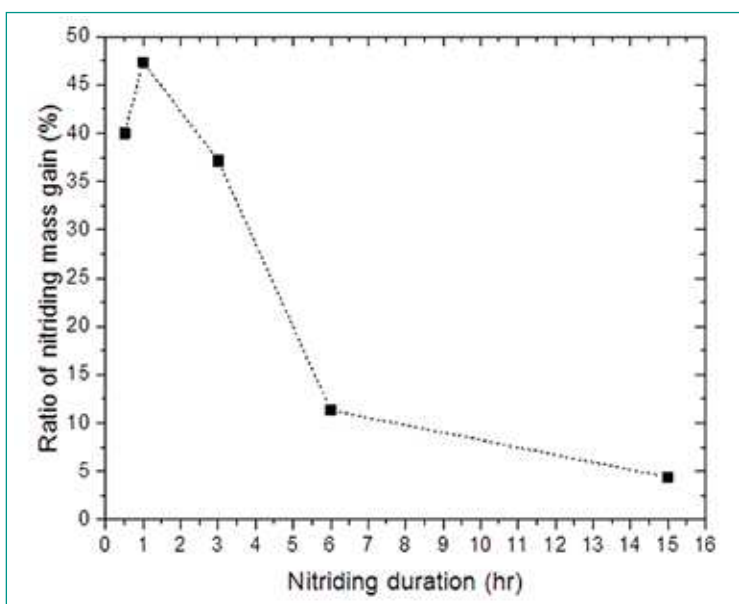Figure 5: *Reaction rates of N₂ with different Zr species*

Figure 6: *The effect of break-away oxidation on nitriding mass gain*

into the metal forming a layer of oxygen stabilized α-Zirconium, αZr(O), between the oxide layer and the Zr metal. Once the sample is exposed to nitrogen, the αZr(O) reacts fast with nitrogen resulting in formation of ZrN. Oxygen released from the oxide due to nitride formation diffuses further into the metal forming new αZr(O). In this region, the nitriding reaction is mainly controlled by the diffusion of nitrogen through the oxide layer, and diffusion of oxygen into the metal to form new αZr(O). It should be noted that the existence of αZr(O) is crucial for the formation of ZrN as it has been shown [6] that the reaction of nitrogen to form ZrN is much faster with αZr(O) than any other Zr and oxygen containing species, Fig. 5.

Break-away region

Break-away takes place when the oxide layer gets thicker than a critical thickness at a specific temperature. Full description of the phenomenon is given in [5]. For subsequent nitriding, it was observed in the separate effect tests in this work, that the break-away oxidation affects the nitriding rate in the first 6 hours of the exposure to nitrogen, Fig. 6. After that, the samples in the non-break-away and break-away regions showed similar nitriding rates. For the model, it can be assumed that αZr(O) is formed on the edges of the cracks which are formed during break-away oxidation, and this results in fast nitriding reaction rate in the beginning of the nitriding. Once the αZr(O) in the cracks is consumed, the nitriding rate will slow down. Consequently, in the break-away region the nitriding phase includes faster and slower nitriding rate.

High temperature region > 1050 °C

Pre-oxidation is traditionally believed to form a protective oxide layer and underneath the oxide layer, αZr(O) is formed in the interface between the oxide and the metal. However, tests by Stuckert and Veshchunov [7] showed that αZr(O) can also form on the outer surface of the oxide layer, Figure 7, as well as on the surface of possible cracks in the oxide. This has been observed to happen in temperatures close to the ones of the high temperature region of the present study. This leads to the hypothesis for the nitride formation at the high temperature region.

Thermogravimetric tests showed two distinctly different nitriding reaction rates at the high temperature region, a very fast nitriding in the beginning of the exposure to nitrogen, and a slower nitriding afterwards. It is assumed that the very fast

254

nitriding takes place when the αZr(O) on the outer surface of the oxide reacts with nitrogen to form ZrN. Also the αZr(O) on the surface of possible cracks may contribute to this fast nitriding. The nitriding rate decreases once the αZr(O) on the surface has been consumed, and nitrogen has to diffuse through the oxide layer to react with the αZr(O) in the interface between oxide and the metal. The absence of oxygen in the exhaust gas in the separate effect tests, as well as integral air ingress tests [8], implies that oxygen which is released from the formation of ZrN is not released from the sample, but diffuses into the metal forming new αZr(O). Therefore, while the production of ZrO_2 stops under starvation of steam and oxygen, the production of αZr(O) continues as long as both ZrO_2 and Zr metal are available [6]. After the first very fast nitriding as a result of reaction of the αZr(O) layer on the outer surface of the oxide, various simultaneous mechanisms participate in the nitriding reaction. The relative importance of them remains to be determined before reaction rates can be implemented in the model.

Analysis of the speciation of Zr–O–N system

Cladding samples were analysed for the speciation of Zr-O-N system after the pre-oxidation and subsequent nitriding using various analysis methods. Especially, the existence of ternary compounds, i.e., Zr-oxynitrides was investigated to assess if these compounds should be included in the nitriding model. For the analysis, the samples were embedded in an epoxy resin, cut, ground, and polished.
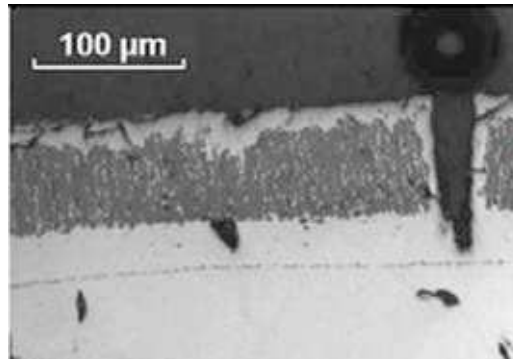
The morphology and surface structure as well as the elemental composition of some of the samples was determined with a scanning electron microscope (SEM) combined with a wave-length dispersive spectroscopy (WDS). The different Zr-O-N phases were analysed with Raman spectroscopy to identify chemical speciation of the samples, and to evaluate the possibility of formation of mixed Zr-O-N phases. Crystalline phases were analysed with X-ray diffraction (XDR), and attempts were made to identify Zr-O-N mixed phases on the sample surface using X-ray photoelectron spectroscopy (XPS).

Raman spectroscopy

Eight samples were prepared for Raman spectroscopy, four at 1000 °C and four at 1200 °C. The pre-oxidation and nitriding times at 1000 °C were 20 min and 15 h, and at 1200 °C 10 s and 30 min, respectively. The collected spectra were compared with three reference samples: i) m-ZrO_2 which was prepared by steam oxidation of Zry-4 at 1200 °C for 15 min, ii) a commercial ZrN powder, and iii) a
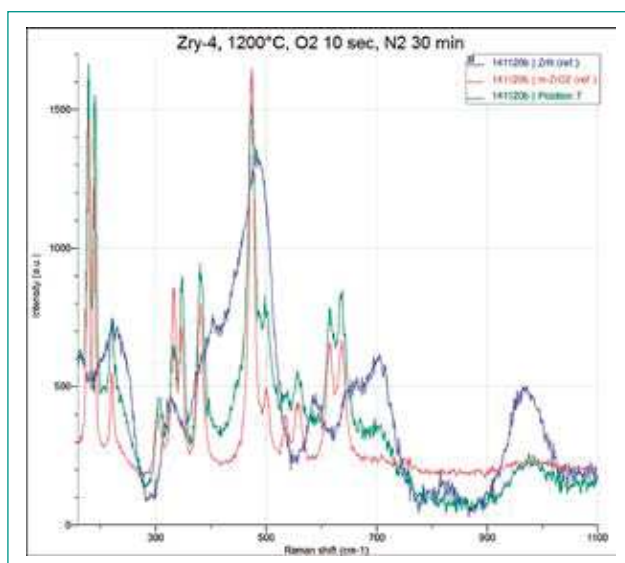
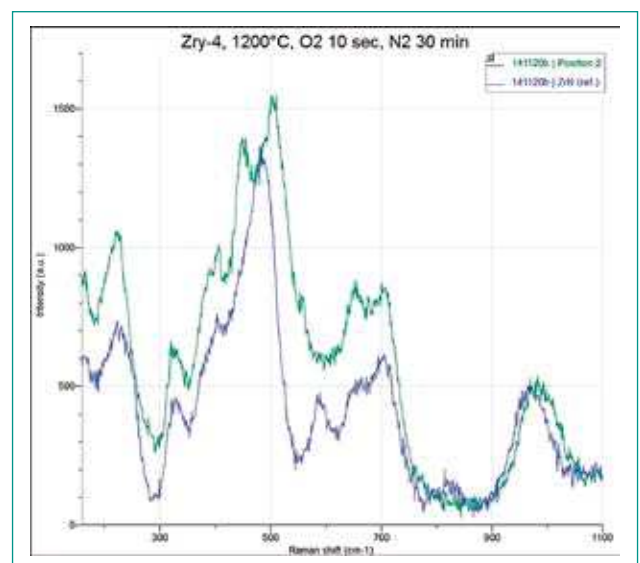**Figure 8:** *Raman spectrum showing a mixture of ZrO_2 and ZrN*

Figure 9: *Raman spectrum showing unidentified peaks*

sample of Zr-oxynitride prepared by an external collaborator. However, it was not confirmed by the analysis that the Zr-oxynitride sample had the desired composition, and therefore it was excluded from the result evaluation. The evaluation was then based on comparing the Raman spectra of the pre-oxidized and nitrided samples with the reference spectra of m-ZrO_2 and ZrN, and identification of the characteristic peaks of both materials in the spectra. The Raman analysis confirmed that the oxide scale formed during pre-oxidation of the samples in the thermo-balance was m-ZrO_2, and the spectra adjacent to the oxide were very similar to the ZrN spectrum. The possible existence of Zr-oxynitrides was investigated by comparing the oxided and nitrided samples with both reference samples. If there is a mixture of m-ZrO_2 and ZrN in the sample, the Raman spectrum would contain peaks of both m-ZrO_2 and ZrN, since crystals of m-ZrO_2 and ZrN are large enough to be detected with Raman. Indeed, many areas in the samples could be identified as a mixture of m-ZrO_2 and ZrN as peaks of both m-ZrO_2 and ZrN were detected in the spectra, Figure 8. However, spectra from some areas showed also unidentified peaks at 452 and 502 cm⁻¹, Figure 9. These peaks indicate the existence of phases not included in the reference samples for m-ZrO_2 and ZrN, for example, Zr-oxynitrides.

**X-ray diffraction and other methods**

X-ray diffraction (XRD) was used to analyse the samples for crystalline compounds. The main aim was to confirm the indication of existence of Zr-oxynitrides detected in the Raman spectra. Optical analysis showed that the possible Zr-oxynitrides would be yellowish in color, and therefore, yellow parts of the samples were selected for further analysis by XRD. The XRD analysis confirmed the existence of both ZrO_2 and ZrN in the samples. In addition, the XRD analysis indicated the existence of $Zr_7N_4O_8$, however, this was a vague indication and not confirmed by further analysis. The conclusion based on the XRD analysis was that the samples contained mainly ZrO_2 and ZrN, however, the existence of small amounts of $Zr_7O_{11}N_2$ could not be excluded.

It should be added that analyses were also carried out using combined scanning electron microscopy (SEM) and energy-dispersive X-ray spectroscopy (EDS) and wave-length dispersive spectroscopy (WDX), as well as X-ray photoelectron spectroscopy (XPS). Whereas these analyses showed the presence of Zr, oxygen and nitrogen in the same areas in the samples, they did not bring conclusive evidence of the existence of Zr-oxynitrides.

Based on all the composition analyses, it was decided that the Zr-oxynitrides would not be included in the nitriding model at this stage, as their presence in the samples could not be exclusively confirmed, and even if present in the samples, the concentration would be minor compared to ZrO_2 and ZrN.

256
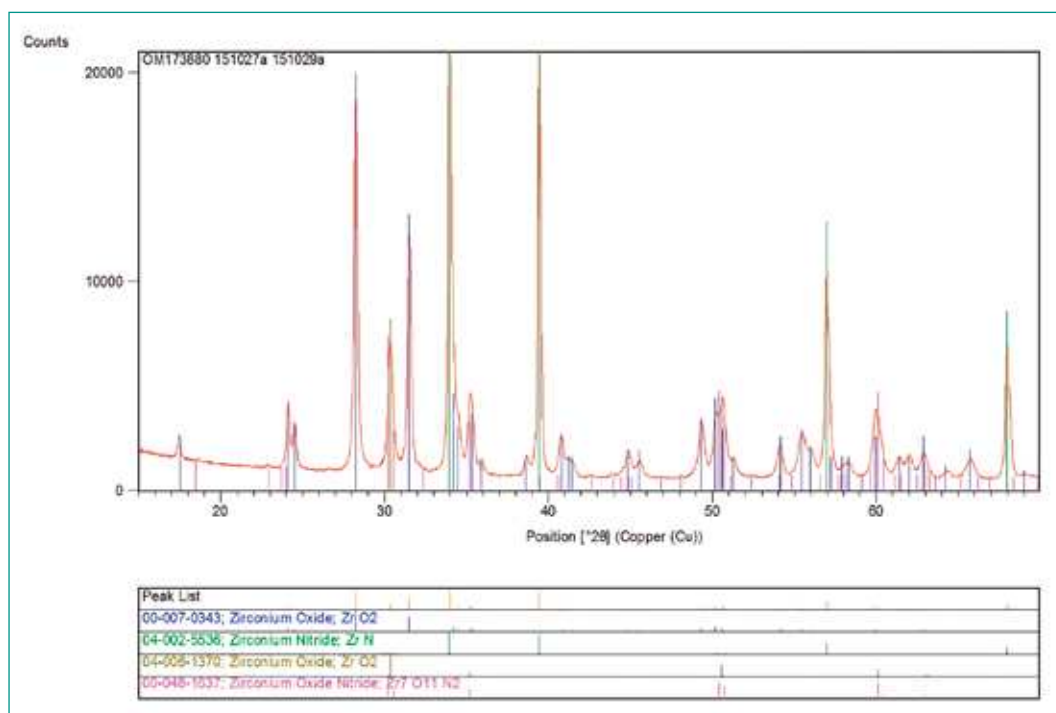
Work carried out in Phase-2

Phase-2 of the project started in the beginning of July 2017. It was foreseen to start Phase-2 by summarizing the available data for cladding pre-oxidation and nitriding, and then writing a stand-alone model for the pre-oxidation – nitriding phases. However, during the data analysis it was concluded that it would be better to write an integral model for nitriding and re-oxidation, i.e., not make a separate nitriding model, as several model elements would be common for the nitriding (including pre-oxidation) and re-oxidation model. Consequently, the first six month of Phase-2 were used to i) re-analyse some of the experimental data, ii) analyse the different phases in the tests, and iii) to determine reactions and reaction rates for the different test phases. The cladding sample mass gain rate during the pre-oxidation was found to follow the known parabolic oxidation rates, Figure 4 [9]. However, it should be noted that the oxidation rate by [9] gives only the total mass gain during oxidation, not the relative fractions of oxygen consumed for formation of ZrO_2 and $\alpha Zr(O)$ which is critical to know in order to determine the amount of $\alpha Zr(O)$ available for fast nitriding. It is presently explored if further experimental data are available and could be used to determine the fraction of ZrO_2 and $\alpha Zr(O)$, or if available equations from literature will be used to determine this ratio.

Nitriding reaction rate was observed to be linear, consisting of first fast nitriding assumed to be a result of reaction of nitrogen with $\alpha Zr(O)$ existing in the samples after pre-oxidation, Figure 11. Fast nitriding was followed by a second, slower nitriding phase, Figure 12. Here data especially at 1000 °C show large scatter, and further analysis will be devoted to determine the main mechanisms which defines the reaction rate. It is presumed that the transport of nitrogen through the oxide – nitride layer is a critical factor in determining the reaction rate, and the structure of the layer may need to be accounted for. In 2018, the work continues by addressing the aforementioned issues, as well as by determining the reaction rates for the re-oxidation phase. It is foreseen that a first version of a stand-alone model for pre-oxidation – nitriting – re-oxidation process be written during 2018. The results will be compared with the composition of the samples after nitriding determined by metallographic analysis combined with image analysis. Further validation of the model is foreseen to be carried out in the following years.
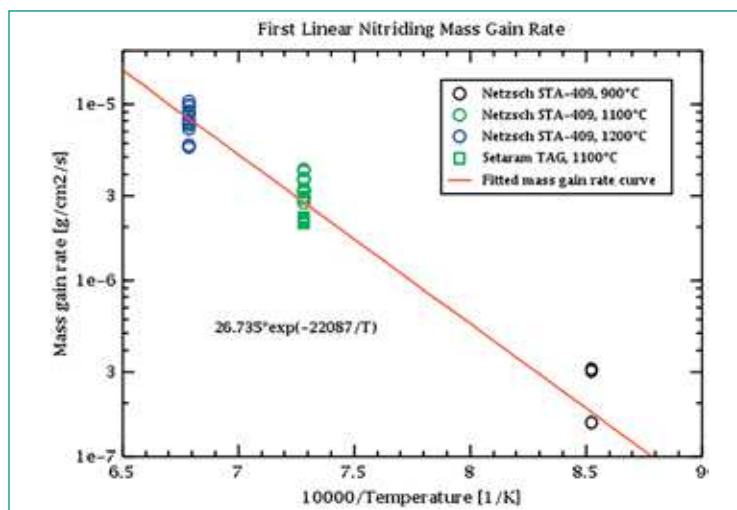

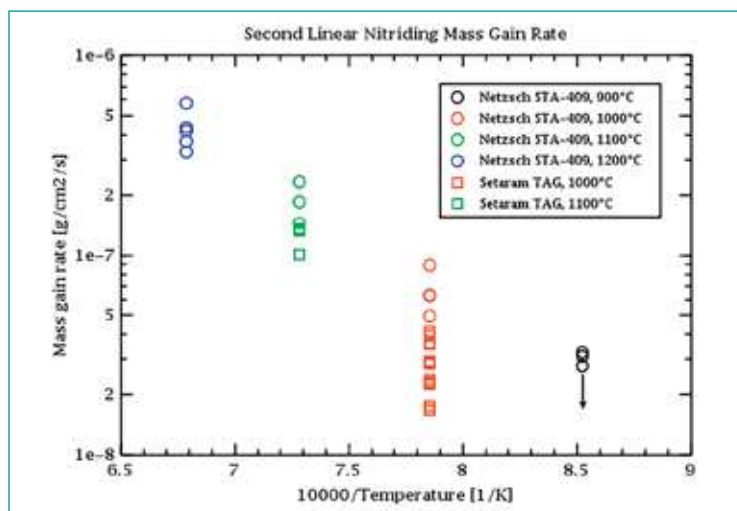Figure 11: *Mass gain rate during first linear nitriding*

Figure 12: *Mass gain rate during second linear nitriding*

National Cooperation

A PhD student works in the analysis of the test results and the model development. He is enrolled at ETHZ and is supervised by Prof. Prasser/ETHZ even though he is not employed by PSI any more.

International Cooperation

A PhD work is performed in collaboration with Karlsruhe Institute of Technology (KIT). The thermogravimetric tests as well as the metallographic analyses were carried out by the PhD student at KIT. The experimental work at KIT is supervised by Dr. Martin Steinbrück. The second supervising professor of the thesis work is Prof. Seifert from KIT. In addition, a close collaboration with M.Steinbrück has been established to perform additional experiments and to deliver data from earlier work relevant to the present project.

257

The model implementation to SCDAP/RELAP5 code has been discussed and agreed with ISS which is the developer of the code. It is foreseen that a scientist from PSI will do the implementation in close collaboration with ISS engineers.

US NRC and Sandia National Laboratories have expressed interest to implement the new model in the severe accident code MELCOR.

Assessment 2017 and Perspectives for 2018

In Phase-1 of the project, nitriding mechanisms of Zircalloy cladding were determined based on thermogravimetric tests in the temperature range 900-1200 °C. It was observed that the nitriding mechanisms were distinctly different in the temperatures below 1050 °C and above this temperature. Reaction mechanisms were postulated for both temperature ranges, and a conceptual model was developed for the cladding nitriding in the presence of air. The final model could not be developed within Phase-1 as foreseen, however, it is foreseen that a combined model for nitriding and re-oxidation of the cladding will be developed in 2018.

In Phase-2, some of the experimental data were re-analysed, and the reaction rates were determined for the pre-oxidation and nitriding phases. Analysis of re-oxidation phase was started and it was decided that formulation and reaction rates used for pre-oxidation can also be used for description of the re-oxidation reactions. Further analysis will be conducted in 2018 with the first stand-alone model for nitriding and re-oxidation foreseen to be made in this year.

Publications

- ▌ *S. Park,* The role of nitrogen during air oxidation, 19th International QUENCH Workshop, KIT, 19–21 November 2013. ISBN 978-3-923704-79-8
- ▌ *S. Park, L. Fernandez-Moguel, M. Steinbrück, J. Birchely, H.-M. Prasser, H.-J. Seifert,* A mechanism of nitridation process in the Zr-O-N system during air oxidation, NuMat 2014: The Nuclear Materials Conferences, 27–30 October 2014, Florida, US.
- ▌ *S. Park,* Overview of the air oxidation kinetic modeling, 20th International QUENCH Workshop, 11–13 November 2014, KIT, Germany. ISBN 978-3-923704-88-0

- ▌ *S. Park, L. Fernandez-Moguel, H.-M. Prasser, J. Birchley, M. Steinbrück, M. Rinke, H.-J. Seifert.* Effect of nitriding during an air ingress scenario. TopFuel 2015: Reactor Fuel Performance.
- ▌ *S. Park, L. Fernandez-Moguel, H.-M. Prasser, J. Birchley, M. Steinbrück, M. Rinke, H.-J. Seifert.* Effect of nitriding and re-oxidation of preoxidized Zry-4. 21st International QUENCH Workshop. 2015. ISBN 978-3-923704-90-3
- ▌ *B. Jäckel, S. Park, L. Fernandez-Moguel* Analysis of Oxidation and Nitriding Experiments of Zircaloy-4 Cladding. 2nd NuFuel Conference, Lecco, Italy, September 4–6, 2017.
- ▌ *B. Jäckel, S. Park, L. Fernandez-Moguel* Progress on Nitriding Modelling for SA codes. CSARP Meeting, September 12–14, 2017.
- ▌ *B. Jäckel, S. Park, L. Fernandez-Moguel* Status Report on Nitriding Model. 23rd QUENCH workshop, Karlsruhe, Germany, October 17–19, 2017.

References

[1] *S.G. Durbin* et al. Spent Fuel Pool Project Phase II: Pre-Ignition and Ignition Testing of a 1x4 Commercial 17x17 Pressurized Water Reactor Spent Fuel Assemblies under Complete Loss of Coolant Accident Conditions. NUREG/CR-7216 (2016).

[2] *J. Birchley, L. Fernandez-Moguel* Simulation of air oxidation during a reactor accident sequence: Part 1 – Phenomenology and model development. Annals of Nuclear Energy 40, 163 (2012).

[3] ENSI Erfahrungs- und Forschungsbericht 2015, Page 225–232.

[4] ENSI Erfahrungs- und Forschungsbericht 2016, Page 227–232.

[5] *J. Birchley, L. Fernandez-Moguel* Annals of Nuclear Energy, 2012

[6] *M. Steinbrück* High-temperature reaction of oxygen-stabilized α-Zr(O) with nitrogen. Journal of Nuclear Materials 447, 46 (2014).

[7] *J. Stuckert, M.S. Veshchunov* Behaviour of Oxide Layer of Zirconium-Based Fuel Rod Cladding under Steam Starvation Conditions. FZKA Report 7373 (2008).

[8] *J. Stuckert et al.,* QUENCH-18 test. 23rd QUENCH workshop, Karlsruhe, October 17–19, 2017.

[9] *H. Uetsuka, P. Hofmann* Reaction Kinetics of Zircaloy-4 in a 25% O_2/75% Ar Gas Mixture Under Isothermal Conditions. KFK Report 3917 (1985).